Ultra-Compact Band-Pass and Band-Stop Tunable Filters Based on Loop-Cascaded Nanobeam Structure

Yuan Wang, Yaotian Zhao, Jinlong Xiang, Xuhan Guo, Jianji Dong, *Senior Member, IEEE*, Xinliang Zhang, *Senior Member, IEEE*, and Yikai Su, *Senior Member, IEEE*

***Abstract*— We propose an ultra-compact band-pass and band-stop filter with bandwidth tunability based on the loop-cascaded nanobeam structure in simulation, with a small coupling region of 41 × 1 μm^2. It features low insertion loss, large bandwidth tunable range and high sidelobe suppression ratio. By two-stage cascading, the bandwidth of the band-pass filter can be adjusted in the range of 6 nm-24 nm. We also experimentally demonstrate the loop-cascaded nanobeam band-pass and band-stop filter with a coupling region of only 17.5 × 1 μm^2.**

***Index Terms*— Silicon photonics, nanobeam, tunable filter, contra-directional coupling.**

I. Introduction

OPTICAL filters are the fundamental components in wavelength-division multiplexing (WDM) systems for routing and selecting wavelengths [1], [2]. In order to meet the more dynamic, gridless and smart-network communication requirements, various optical tunable filters have been demonstrated on a silicon-on-insulator (SOI) platform. To date, many tunable filters have been demonstrated, mainly including those based on microring resonators (MRRs) [3] and Mach Zehnder interferometers (MZIs) [4], [5]. They either have the advantages of high-quality factor (Q) or good fabrication tolerance. However, these devices exhibit limited bandwidth (BW) (usually less than 10 nm) or free spectral ranges (FSRs), which may not well address the demands of some requirements for high-capacity transmission applications. To solve these problems, recently, contra-directional couplers (contra-DCs) have been proposed as an effective method for optical filters without FSR [6], [7]. This kind of devices also has merits of broad BW with flat-tops, small insertion losses (IL) and low crosstalk. However, they usually occupy large footprints on a SOI wafer. Subsequently, compact and pass-band BW tunable filter based on subwavelength grating (SWG) assisted contra-DCs [8] have been demonstrated. However, the stop-band BW cannot be tuned simultaneously when two SWG filters are cascaded.

Very recently, nanobeam structure, a 1D photonic crystal waveguide (PhCW), has been studied for optical filters due to their ultra-compact feature [9]–[11]. The nanobeam structure can form the photonic mini-stopband (MSB) between the fundamental mode and the higher-order mode, which can be utilized to implement the band-stop filter function [9]. As the periodic holes of nanobeam are equivalent to periodic dielectric perturbations in the contra-DC, there is also contra-directional coupling between the fundamental mode and the higher-order mode, hence nanobeam structure can be delicately utilized as the band-pass filter as well. If combining the advantages of nanobeam features and contra-DC function together, the passing light (fundamental mode) and reverse coupled light (high-order mode) can form band-pass and band-stop filters respectively in the same waveguide.

In this letter, we propose an ultra-compact, BW-tunable optical filter based on a loop-cascaded nanobeam structure with a small coupling region of 41 × 1 μm^2. The BWs of the band-pass filter and band-stop filter can be tuned simultaneously. By two-stage cascading, the 3 dB BW of the band-pass filter can be continuously tuned from 24 nm with a high out-of-band contrast of 42 dB to 6 nm with an out-of-band contrast of 19 dB. We also experimentally demonstrate the loop-cascaded nanobeam based band-pass and band-stop filters with a coupling region of only 17.5 × 1 μm^2.

II. Principle and Simulations

The schematic diagram of our proposed single nanobeam filter is shown in Fig. 1(a). It consists of a TE_0 to TE_2 mode demultiplexer, periodic holes and the tapered multimode waveguide. We use the asymmetric directional coupler (ADC) as the mode demultiplexer for high-order modes [12]. The 1D PhCW nanobeam structure consists of a central multimode waveguide with the width W of 1 μm, and the period of the hole Λ of 355 nm. The widths of the waveguides (w_1, w_2),

Manuscript received July 27, 2021; accepted August 16, 2021. Date of publication August 24, 2021; date of current version August 31, 2021. This work was supported in part by the National Key Research and Development Program of China under Grant 2019YFB2203104, in part by the Natural Science Foundation of China under Grant 61805137 and Grant 61835008, in part by the Natural Science Foundation of Shanghai under Grant 19ZR1475400, and in part by the Open Project Program of Wuhan National Laboratory for Optoelectronics under Grant 2018WNLOKF012. *(Corresponding author: Xuhan Guo.)*

Yuan Wang, Yaotian Zhao, Jinlong Xiang, Xuhan Guo, and Yikai Su are with the State Key Laboratory of Advanced Optical Communication Systems and Networks, Department of Electronic Engineering, Shanghai Jiao Tong University, Shanghai 200240, China (e-mail: wangyuan666@sjtu.edu.cn; zhaoyaotian@sjtu.edu.cn; xjl515030910046@sjtu.edu.cn; guoxuhan@sjtu.edu.cn; yikaisu@sjtu.edu.cn).

Jianji Dong and Xinliang Zhang are with Wuhan National Laboratory for Optoelectronics, School of Optoelectronic Science and Engineering, Huazhong University of Science and Technology, Wuhan, Hubei 430074, China (e-mail: jjdong@mail.hust.edu.cn; xlzhang@mail.hust.edu.cn).

Color versions of one or more figures in this letter are available at https://doi.org/10.1109/LPT.2021.3107307.

Digital Object Identifier 10.1109/LPT.2021.3107307

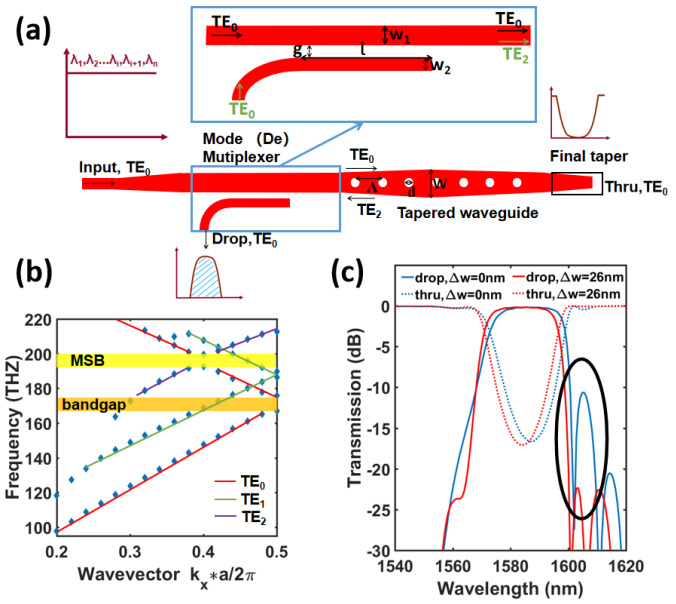

Fig. 1. (a) Schematic diagram, (b) Band structure and (c) Simulated results of the proposed single nanobeam filter.

coupling length (l) and gap (g) are 1290 nm, 406 nm, 21.3 μm and 200 nm respectively. Figure 1(b) shows the band structure of the TE-polarized Bloch modes in the nanobeam calculated using the three-dimensional finite-difference time-domain (3D-FDTD) method. We can obverse an obvious MSB between TE_0 and TE_2, hence the input TE_0 mode in the MSB will be coupled to the backward TE_2 mode in the multimode waveguide.

The working principle of our proposed structure follows the coupled mode theory [8], [13], when a continuous wave (CW) light TE_0 is launched into the input port, the undesired co-directional coupling is suppressed due to the phase mismatching between the TE_0 and TE_2 mode. The light that satisfies the phase-matching condition as

$$\frac{\lambda_c}{\Lambda} = n_1 + n_2 \tag{1}$$

can be reversely coupled, where n_1 and n_2 represent the effective indices of the TE_0 and TE_2, Λ is the period of the hole and λ_c is the central wavelength. The transmission spectrum at the through (thru) port presents a band-stop response. The reflected TE_2 light passes through the ADC and is converted back to TE_0, presenting a band-pass response at the drop port. The BW can be written as:

$$\Delta\lambda = \frac{2\lambda_0^2}{\pi(n_1 + n_2)}|\kappa| \tag{2}$$

$$\kappa = \frac{\omega}{4}\iint E_1^*(x,y)\cdot\Delta\varepsilon_1(x,y)E_2(x,y)dxdy \tag{3}$$

where κ is the coupling coefficient, ω is the frequency of the light, E_1 and E_2 are the amplitude of two coupled modes, $\Delta\varepsilon_1$ is the first-order Fourier-expansion coefficient of the periodic dielectric perturbation.

To suppress sidelobes of the pass-band, the diameter of the holes is also apodized using a Gaussian function as follows:

$$d = d_0\exp(-a(n-0.5N)^2/(0.5N)^2) \tag{4}$$

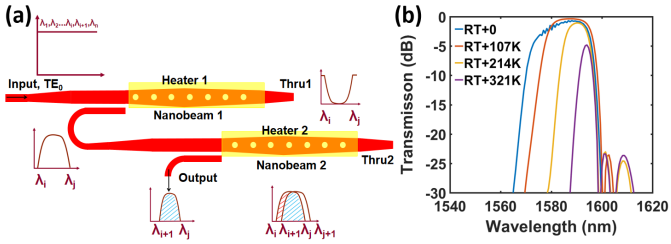

Fig. 2. (a) Schematic diagram and (b) Simulated results of the proposed cascaded nanobeam filter.

where n is the sequence of holes, N is the total number of holes, and a is the apodization index. We need to take proper values of N and a to ensure that the performance of the filter is balanced and relatively good. Here, we take $N = 118$ and $a = 5$. When the waveguide of the nanobeam is straight waveguide ($\Delta w = 0$), the simulated performances of the filter are shown in Fig. 1(c) (blue-solid line). We can see that the sidelobe on the left side of the spectrum is well suppressed, while the right-side sidelobe is still poor due to apodization induced equivalent refractive index change along the propagation direction. In order to compensate that, a two-side tapered waveguide is used. The width of the central multimode waveguide remains unchanged (1000 nm), then we linearly taper the waveguide towards the two sides to 974 nm ($\Delta w = 26$nm), we can see that the sidelobes on both sides of the central wavelength can be well suppressed, as shown in Fig. 1(c) (red-dot line). After the optimization, we can achieve relatively good performance of both the band-pass and band-stop filtering functions from the nanobeam structure. The IL of the bandpass filter is less than 0.1 dB, with a sidelobe suppression ratio (SLSR) larger than 23 dB. Due to the large coupling coefficient between TE_0 mode and TE_2 mode in the same multimode nanobeam waveguide, the coupling length is only 41 μm.

Then, a tunable filter composed of a two-stage cascaded nanobeam filter is proposed as shown in Fig. 2(a). The drop port of one nanobeam filter is connected to the input port of another identical nanobeam filter. The final drop port response could be effectively regarded as the spectrum overlap of the two nanobeam filters. To achieve tunable BW, we tune the nanobeam 2 independently. We evaluate the temperature dependence using $d_{neff} = dn_{Si}/dT \times d_{neff}/dn_{Si} \times dT$ [5] from room temperature (RT). For nanobeam 2, the input signal is the passband from the drop port of nanobeam 1. We set the band range of the passband as (λ_i, λ_j). Due to the red shift of its thermal tunable band, we adjust the band range $(\lambda_{i+1}, \lambda_{j+1})$ to satisfy the coupling condition of nanobeam 2, which leads to the output port presenting as a pass-band of $(\lambda_j, \lambda_{i+1})$. When we increase the power of heater 2, the pass-band becomes narrower and achieves the BW tunability. As shown in Fig. 2(b), continuous tuning of the 3 dB BW from 24 nm down to 6 nm is observed. However, as the bass-band edges are determined by another drop filter during the tuning process, the SLSR degrades from 42 dB down to 19 dB. Note that the response spectra of the drop filter are not the ideal rectangle shape, so the ILs are observed to increase during the thermal tuning.

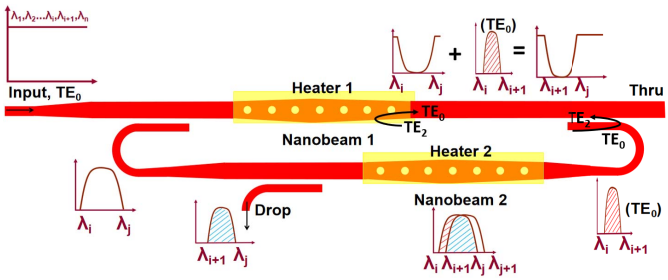

Fig. 3. Schematic diagram of the proposed loop cascaded nanobeam filter.

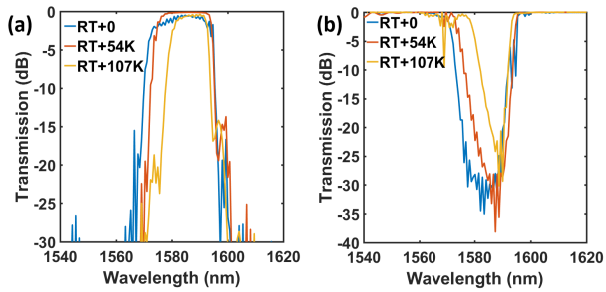

Fig. 4. Simulation results of the proposed loop cascaded nanobeam filter: (a) drop port, (b) thru port.

In order to tune the BWs of the band-pass and band-stop filters synchronously, we further propose a loop-cascaded nanobeam filter, as shown in Fig. 3.

We make the same ADC mode (de) multiplexer of TE_0 to TE_2 from the left side of nanobeam1 symmetrical to the right side of nanobeam 1. In this way, the band-pass signal of thru 2 (λ_i, λ_{i+1}; TE_0) is added to the nanobeam 1 through the ADC. As the wavelengths (λ_i, λ_{i+1}) are within the coupling condition wavelength range of nanobeam 1, the (λ_i, λ_{i+1}; TE_2) is coupled to TE_0 in the forward direction. As a result, the BW range of drop and thru port are both (λ_{i+1}, λ_j). Therefore, the BW in the drop port and thru port can be tuned simultaneously. In order to mitigate the interference effect between the two signals, it is necessary to ensure that the coupling length is long enough. Therefore, the coupling length is increased from 41 μm to 80 μm, and the number of holes is increased from 120 to 230. The simulation results are shown in Fig. 4.

From Fig. 4, we can see that in our designed loop-cascaded nanobeam filter, with the increase of heater 2 power, the band-pass filter (drop port) and the band-stop filter (thru port) can be tuned simultaneously. The BWs of the band-pass filter and band stop filter are tuned synchronously in the range of 14 nm (RT + 107K) to 24 nm (RT). In the process of thermal tuning, the SLSR of the band-pass filter is all above 15 dB, the extinction ratio (ER) of the band-stop filter is above 30 dB, and the ILs of band-pass and band-stop filters are below 0.1 dB. However, due to the phase difference between the thru port of nanobeam 1 and nanobeam 2, the band-stop filter shows some ripples.

III. Fabrication, Experimental Setup and Results

The proposed devices are fabricated on a SOI wafer consisting of a 220-nm-thick top silicon layer and a 3-μm-thick buried oxide layer. The fabrication process mainly includes the electron-beam lithography (EBL) followed by the inductively coupled plasma (ICP) process on the silicon layer. In order to achieve better fabrication tolerance, we increase the diameter of the holes while shortening the coupling length, which will make the BW wider. And the following parameters are used: the diameter of the central hole $d_0 = 120$ nm, the period of the hole $\Lambda = 355$ nm, the apodization index $a = 2.5$. The width of the tapered waveguide in the middle is 1000 nm, and the width of the two sides is 940 nm. Finally, a 2-μm-thick silica layer is deposited on the structure as upper cladding by plasma-enhanced chemical vapor deposition (PECVD).

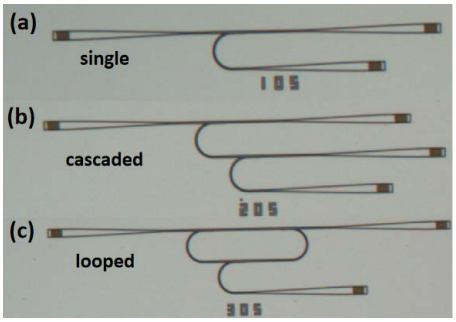

Fig. 5. Microscope photos of the devices: (a) single nanobeam, (b) cascaded, and (c) loop structure.

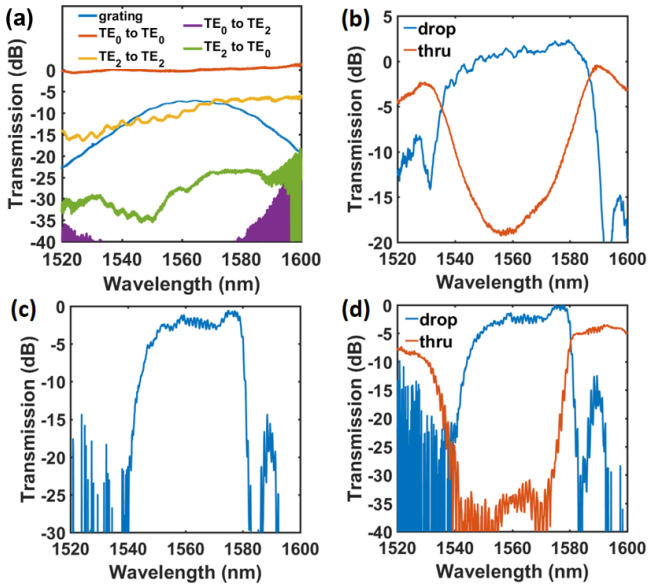

Fig. 6. Spectral response of the: (a) reference grating and reference ADC, (b) single nanobeam filter after normalization, (c) cascaded nanobeam filter after normalization, (d) loop-cascaded nanobeam filter after normalization.

Figure 5 depicts the microscope photos of the devices. The scanning electron microscope (SEM) images of the device details are not available due to the thick silica cladding. A tunable laser source (Keysight 81960A) and an optical power meter (Keysight N7744A) are used to characterize the spectra of the devices. It should be noted that these devices are fabricated without heaters, so the BW tunability are not demonstrated here.

The experimental results are shown in Fig. 6. The spectra responses of the grating and the loss and the crosstalk of the ADC-based mode demultiplexer are shown in Fig. 6(a). Figure 6(a) indicates that the grating couplers have relatively

TABLE I
RECENT RESULTS WITH ON-CHIP TUNABLE FILTERS BASED ON CONTRA-DCS

Publication	Filter Type	Contra-coupling Length	Tunable (pass band)	BWIL	SLSR
J. St-Yves *et al.* [6]	Cascaded GACDCs	312 μm	~5.4 nm	< 0.5 dB	15~55 dB
M.T.Boroojerdi *et al.*[7]	Cascaded GACDCs	312/318 μm	10.6 nm	2.6 dB	31 dB (max)
K. Wang *et al.* [8]	Cascaded SWG	100 μm	6 nm	~ 2 dB	15~25 dB
J. Jiang *et al.* [14]	Cascaded Gratings	500 μm	12 nm	< 2 dB	18~30 dB
This Work (Sim.)	Cascaded nanobeam	41 μm	18 nm	~ 1.1 dB	19~42 dB
This Work (Expt.)	Cascaded nanobeam	17.5 μm	N.A.[#1]	~0.4dB[#2]	14 dB

#1 The devices are fabricated without heaters, so the BW tunability are not demonstrated here.
#2 Normalized by the grating couplers and ADCs.

good performance. Unfortunately, the performance of ADCs is not as good as expected due to the fabrication inaccuracies, and its spectra have some ripples and relatively large IL. Here we normalize filter responses with both the grating couplers and the ADCs to reflect the response of the proposed structures themselves.

Figure 6(b) shows the normalized spectra of the single nanobeam filter, and both band-pass and band-stop filters can be realized in the coupling region of only 17.5 × 1 μm^2. Since the ADC-based mode (de)multiplexers are sensitive to fabrication inaccuracies, the performances of same mode (de)multiplexers are slightly different, causing the normalized spectra of the single nanobeam filter slightly higher than 0 dB in the wavelength range from 1560nm to 1580 nm. The SLSR of the band-pass filter is 10 dB, the ER of the band-stop filter is 18 dB and the BW is 53 nm. Figure 6(c) shows the normalized spectra of cascaded nanobeam structure, the SLSR of the band-pass filter can be higher compared with a single structure (~14 dB), the IL is 0.4 dB and the BW is 41 nm. Figure 6(d) shows the normalized spectra of the loop-cascaded structure, the ER of the band-stop filter can be improved compared with a single structure (~40 dB) with the SLSR of the band-pass filter of 10 dB, the IL is only 0.1 dB and the BW is 40 nm.

IV. CONCLUSION

The comparison between our work and recent published tunable filters based on contra-DCs structures is shown in Table 1, which indicates that our proposed loop-cascaded nanobeam tunable filter has the shortest coupling length without performance compromised a lot, and the length of the coupling region of our nanobeam filter is only 17.5 μm, to the best of our knowledge, these are the shortest contra-coupling lengths among the current tunable filters.

In summary, an ultra-compact BW tunable filter based on the loop-cascaded nanobeam structure is proposed. The BW of the band-pass filter and band-stop filter can be tuned simultaneously. Thanks to the large coupling coefficient between TE_0 and TE_2 in the same nanobeam multimode waveguide, the coupling region is only 41 × 1 μm^2. The SLSR is improved by employing the taper waveguides with Gaussian apodized hole diameters in the nanobeam structre. By two-stage cascading, the BW of the band-pass filter can be adjusted in the range of 6 nm to 24 nm. We also experimentally demonstrate a band-pass and band-stop filter based on loop-cascaded nanobeam structure with a coupling region of only 17.5 × 1 μm^2, the ER of the band-stop filter is 40 dB, the SLSR of the band-pass filter is 10 dB, the IL is only 0.1 dB and the BW is 40 nm. The compact size and flexible tunability of BW makes the device a very attractive candidate for dynamic WDM systems in the future.

ACKNOWLEDGMENT

The authors thank the Center for Advanced Electronic Materials and Devices (AEMD) of Shanghai Jiao Tong University (SJTU) for the support in device fabrications.

REFERENCES

[1] P. Dong, Y. K. Chen, G. H. Duan, and D. T. Neilson, "Silicon photonic devices and integrated circuits," *Nanophotonics*, vol. 3, no. 4, pp. 215–218, Aug. 2014.
[2] D. Liu, H. Xu, Y. Tan, Y. Shi, and D. Dai, "Silicon photonic filters," *Microw. Opt. Technol. Lett.*, vol. 63, no. 9, pp. 2252–2268, Sep. 2021.
[3] F. Horst, W. M. J. Green, S. Assefa, S. M. Shank, Y. A. Vlasov, and B. Offrein, "Cascaded Mach–Zehnder wavelength filters in silicon photonics for low loss and flat pass-band WDM (de-)multiplexing," *Opt. Exp.*, vol. 21, no. 10, pp. 11652–11658, May 2013.
[4] Y. Su, Y. Zhang, C. Qiu, X. Guo, and L. Sun, "Silicon photonic platform for passive waveguide devices: Materials, fabrication, and applications," *Adv. Mater. Technol.*, vol. 5, no. 8, pp. 1–19, Aug. 2020.
[5] Y. Zhao, X. Wang, D. Gao, J. Dong, and X. Zhang, "On-chip programmable pulse processor employing cascaded MZI-MRR structure," *Frontiers Optoelectron.*, vol. 12, no. 2, pp. 148–156, Jun. 2019.
[6] J. St-Yves, H. Bahrami, P. Jean, S. LaRochelle, and W. Shi, "Widely bandwidth-tunable silicon filter with an unlimited free-spectral range," *Opt. Lett.*, vol. 40, no. 23, pp. 5471–5474, Dec. 2015.
[7] M. T. Boroojerdi, M. Ménard, and A. G. Kirk, "Wavelength tunable integrated add-drop filter with 10.6 nm bandwidth adjustability," *Opt. Exp.*, vol. 24, no. 20, pp. 22865–22874, Oct. 2016.
[8] K. Wang *et al.*, "Ultracompact bandwidth-tunable filter based on subwavelength grating-assisted contra-directional couplers," *Frontiers Optoelectron.*, early access, 2020. [Online]. Available: https://link.springer.com/article/10.1007/s12200-020-1056-5#citeas, doi: 10.1007/s12200-020-1056-5.
[9] Q. Huang, K. Jie, Q. Liu, Y. Huang, Y. Wang, and J. Xia, "Ultra-compact, broadband tunable optical bandstop filters based on a multi-mode one-dimensional photonic crystal waveguide," *Opt. Exp.*, vol. 24, no. 18, pp. 20542–20551, Sep. 2016.
[10] M. Manuel, O. Hideaki, and N. Hirochika, "Silicon optical filter with transmission peaks in wide stopband obtained by anti-symmetric photonic crystal with defect in multimode waveguides," *Opt. Exp.*, vol. 26, no. 2, pp. 1841–1850, Jan. 2018.
[11] A. Li, J. Davis, and Y. Fainman, "Ultra compact Bragg grating devices with broadband selectivity," *Opt. Lett.*, vol. 45, no. 3, pp. 644–647, Feb. 2020.
[12] D. Dai, J. Wang, and Y. Shi, "Silicon mode (de)multiplexer enabling high capacity photonic networks-on-chip with a single-wavelength-carrier light," *Opt. Lett.*, vol. 38, no. 9, pp. 1422–1424, May 2013.
[13] G. Lifante, *Integrated Photonics: Fundamental*, 2nd ed. Madrid, Spain: Universidad Autonoma de, 2003, pp. 116–121.
[14] J. Jiang *et al.*, "Broadband tunable filter based on the loop of multimode Bragg grating," *Opt. Exp.*, vol. 26, no. 1, pp. 559–566, Jan. 2018.